Chemistry & Biology
Article

Direct Measurement of Cathepsin B Activity in the Cytosol of Apoptotic Cells by an Activity-Based Probe

Matthew R. Pratt,[1,3,*] Matthew D. Sekedat,[2] Kyle P. Chiang,[1] and Tom W. Muir[1,*]
[1]Laboratory of Synthetic Protein Chemistry
[2]Laboratory of Mass Spectrometry and Gaseous Ion Chemistry
The Rockefeller University, New York, NY 10065, USA
[3]Present address: Department of Chemistry, University of Southern California, Los Angeles, CA 90089, USA
*Correspondence: matthew.pratt@usc.edu (M.R.P.), muirt@rockefeller.edu (T.W.M.)
DOI 10.1016/j.chembiol.2009.07.011

SUMMARY

Cells control their own death through a program termed apoptosis, which is indispensable for development and homeostasis in all metazoans. Lysosomal cysteine proteases are not normally thought of as participating in apoptosis; however, recent reports have shown that the cathepsin proteases can be released from the lysosome during apoptosis, where they can participate in cell death. We report here the development of an activity-based probe that, under optimized conditions, reports on cathepsin B activity only in apoptotic cells by reading out the release of cathepsin B from the lysosomes. Biochemical characterization of apoptosis in cells from cathepsin B null mice shows delayed and suboptimal activation of caspases. Our data further supports a role for cathepsin B in the cytosol as a positive regulator of a cell death feed-forward loop and provides a chemical tool for future investigations.

INTRODUCTION

Apoptosis is a tightly regulated form of programmed cell death that plays an essential role in the development and homeostasis in all metazoans (Danial and Korsmeyer, 2004; Rathmell and Thompson, 2002; Zheng et al., 1999). Deficiency in apoptosis is a feature of cancer and autoimmune diseases, whereas improper overactivation of this death program is linked to neurodegenerative disorders (Green and Evan, 2002; Hanahan and Weinberg, 2000; Vaux and Flavell, 2000; Yuan and Yankner, 2000). Two major apoptotic pathways exist in cells, the intrinsic pathway, which senses cellular stress, and the extrinsic pathway, which is induced by extracellular signals such as Fas binding to its cognate death receptor (Riedl and Shi, 2004). Central to both pathways is the cascading activation of a family of cysteine proteases know as the caspases, which are synthesized as inactive zymogens. Upon activation by cross-autoprocessing through dimer- or oligomerization, initiator caspases (caspase-8, -9, and -10) cleave and thereby activate the effector caspases (caspase-3, -6, and -7), which then go on to deactivate, and in some cases activate, numerous cellular targets by proteolytic processing after key aspartate residues (Dix et al., 2008; Mahrus et al., 2008).

Current methods for visualizing these cascades depend heavily on antibodies to detect full-length and/or cleaved, therefore presumably activated, caspases. However, there is evidence that proteolytic cleavage is not always necessary for activation (Stennicke et al., 1999), and endogenous protein inhibitors exist that control caspase activity through a variety of mechanisms including by binding to the processed forms of the enzymes (Deveraux et al., 1999; Riedl and Shi, 2004). Adding to the complexity, some models of apoptosis are dependent on the release of lysosomal proteases known as cathepsins that may act through caspase-dependent or independent mechanisms (Foghsgaard et al., 2001; Guicciardi et al., 2000, 2001; Salvesen, 2001; Turk et al., 2002; Vancompernolle et al., 1998; Yeung et al., 2006). Because of these complications, small molecule inhibitors and substrates targeted against apoptosis-linked proteases have emerged as attractive alternatives to ascertain function. Although current commercially available reagents lack specificity (Kato et al., 2005a), great progress has been made in this area by the recent development of highly selective activity-based probes (ABPs) for caspases-3, -7, and -8 (Berger et al., 2006). These probes have, for instance, allowed for the identification of a novel pathway for caspase-7 activation (Denault et al., 2006).

Here, we describe the development of a cell-permeable ABP originally designed for the monitoring of caspase activity. We utilized a previously developed acyloxymethyl ketone warhead targeted by the general caspase recognition sequence Glu-Val-Asp (Berger et al., 2006; Kato et al., 2005a, 2005b). The cell permeability of our probe was engendered through the use of a two-step labeling procedure in which a bioorthogonal coupling reaction was used to attach a biotin handle to the APB after cell lysis (Figure 1A). Unexpectedly, we find that the conditions of our labeling protocol allow for either the detection of the effector caspases or the selective monitoring of the cysteine protease cathepsin B (CatB). CatB belongs to an 11 member family of cysteine proteases that are typically localized to lysosomal compartments where it primarily contributes to protein turnover. Dysregulation of the cathepsins is linked to a variety of diseases including cancer (Jedeszko and Sloane, 2004; Mohamed and Sloane, 2006), osteoporosis

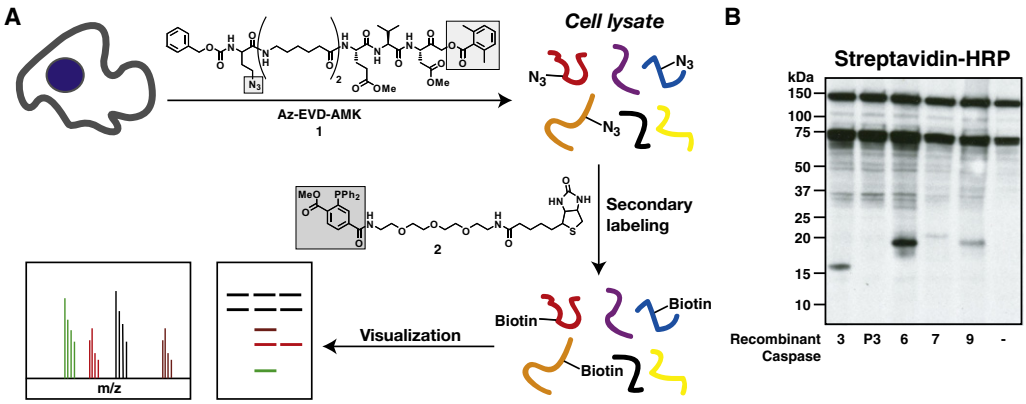

Figure 1. Activity-Based Probe Profiling and Labeling of Recombinant Caspase

(A) Outline of activity-based probe profiling. Apoptotic cells are treated with probe **1**, where it will covalently modify proteins based on their endogenous activities. After cell lysis, the azide handle of **1** will be biotinylated in a secondary labeling step, namely, the Staudinger ligation. Biotinylated proteins can then be analyzed via western blotting and mass spectrometry.

(B) Two-step labeling of recombinant caspases in a complex proteome. Recombinant caspases were added to MCF7 lysates and subsequently labeled with probe **1**. Staudinger ligations were performed with **2**, followed by analysis by streptavidin blotting. Expected molecular weights: caspase-3 (17 kDa), caspase-6 (19 kDa), caspase-7 (19 kDa), caspase-9 (18 kDa), and procaspase-3 (35 kDa). Bands at ~75 and 100 kDa are endogenously biotinylated proteins.

(Saftig et al., 1998), and immunological defects resulting from inefficient major histocompatibility class II antigen presentation (Shi et al., 1999). In addition to its role in lysosomal protein degradation, CatB is also secreted from certain cancer cells where it has been implicated in their detachment and migration (Gocheva et al., 2006; Roshy et al., 2003; Schraufstatter et al., 2003).

Cytosolic relocalization of CatB has been shown to be important in cell death (Kirkegaard and Jaattela, 2009). Lysosomal release of CatB has previously been observed upon stimulation of the extrinsic pathway of apoptosis (Foghsgaard et al., 2001; Guicciardi et al., 2000, 2001). Moreover, this release is implicated in the cross-activation of caspase-9 by caspase-8, thereby linking the extrinsic and intrinsic apoptotic pathways (Guicciardi et al., 2000). In addition, drugs such as bortezomib and granulysin and exposure to UVA/B light have been shown to permeabilize lysosome membranes and induce cathepsin-dependent cell death (Bivik et al., 2006; Droga-Mazovec et al., 2008; Yeung et al., 2006; Zhang et al., 2009). However, the extent of proteolytic activity CatB retains after this translocation event in living cells is less clear or whether CatB release is also a feature of cell death initiated through the intrinsic apoptotic pathway. Our labeling data show that CatB is active in the cytosol of intact cells following stimulation of both the intrinsic and the extrinsic pathways. In the case of the intrinsic pathway, this change in CatB activity is dependent on caspase-9. In addition, intrinsic caspase activation in CatB null cells was both delayed and suboptimal. CatB has been shown in the examples above to induce the release of cytochrome *c* from mitochondria, the first step in caspase-9 activation, and our own biochemical studies indicate that CatB can cleave caspase substrate sequences at cytosolic pH. The development of our cell-permeable and selective probe allowed us to uncover a positive regulatory role for CatB in a feed-forward loop during the intrinsically activated cell death program through one of the two mechanisms outlined above.

RESULTS

Labeling of Recombinant Caspases

We synthesized azide-containing probe **1** (see Scheme S1 available online; Figure 1A) and set out to characterize its activity against the family of caspase proteases. We first examined its ability to label recombinant caspases in a complex cell lysate. Recombinant active caspase-3, -6, -7, and -9, as well as inactive zymogen of caspase-3 (p3) were added separately in equal amounts to cell lysate derived from MCF7 cells. MCF7 cells lack caspase-3 and have very low levels of endogenous caspase activity, providing a suitable background (Yang et al., 2001). Probe **1** (300 nM) was then added and lysate was labeled for 30 min. Excess probe was then removed and phosphine-biotin **2** (250 μM; Figure 1A) was added to biotinylate reactive alkyl azides via the Staudinger ligation (Lin et al., 2005; Saxon and Bertozzi, 2000). After 2 hr at 37°C the secondary labeling reaction was terminated by precipitation and biotinylation was accessed by streptavidin blotting (Figure 1B). All recombinant active caspases were labeled, whereas, as expected, inactive full-length capase-3 remained untouched by the probe (Figure 1B).

Labeling in Living Cells

Next we analyzed the ability of **1** to label caspases in intact cells undergoing apoptosis. Toward this end, NIH 3T3 cells were treated with staurosporine (1 μM) or DMSO vehicle for 3 hr and were then treated with probe **1** (300 nM) for 30 min. The cells were harvested, washed thoroughly, lysed, and reacted with phosphine-biotin **2** as above. Streptavidin blotting revealed the presence of a single biotinylated protein band at a molecular weight of ~30 kDa in apoptotic cells but not healthy cells (Figure 2A). This selectivity is diminished when the proteome is labeled with **1** after lysis (Figure 2A). Note that when higher concentrations of **1** (5–50 μM) were used, we observed this same, labeled protein band in nonapoptotic cells (Figure S1A).

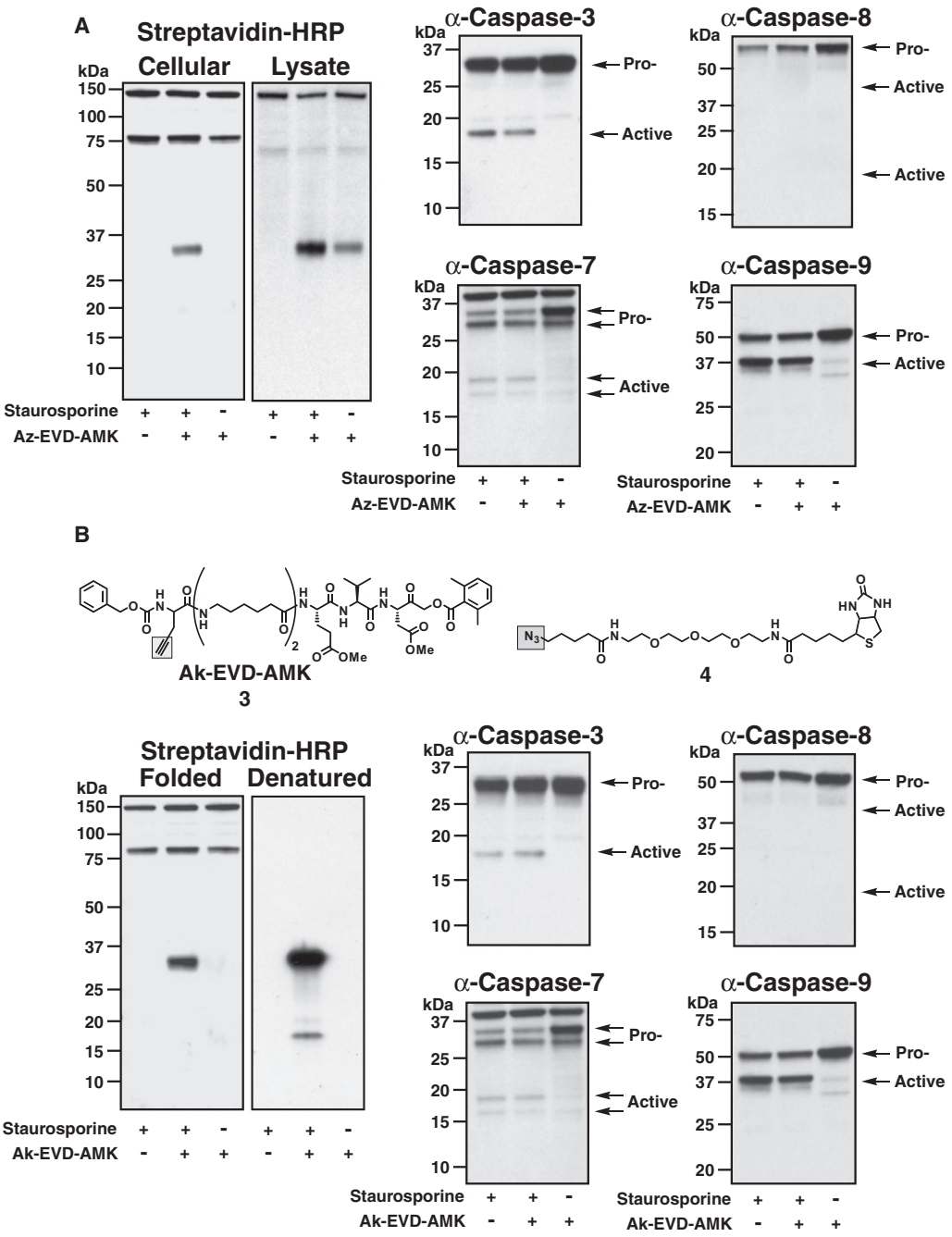

Figure 2. Probe Labeling of Intact Cells

(A) Labeling of intact cells and cell lysates by probe **1**. NIH 3T3 cells were treated with staurosporine (1 μM) or DMSO vehicle. In the case of cellular labeling, probe **1** (300 nM) was added, followed by lysis and biotin modification with **2** via Staudinger ligation. For lysate modification, cells were lysed and then treated with **1** (300 nM) followed by reaction with **2**.

(B) Labeling of intact cells by the alkyne-bearing probe **3**. NIH 3T3 cells were again treated with staurosporine (1 μM) or DMSO vehicle. Probe **3** (300 nM) what then added to the cells, followed by lysis and copper catalyzed cycloaddition chemistry with azide biotin **4**. In both cases probe labeling was analyzed by streptavidin blotting. Caspase activation was monitored by western blotting for cleavage from inactive proenzymes to active enzymes. Endogenous caspase-9 differs in weight from recombinant caspase-9 due to extra domains involved in its activation.

Thus, there is a concentration threshold (~1 μM) below which the visualization of this protein appears to be apoptosis dependent. Surprisingly, the molecular weight of this biotinylated protein was inconsistent with either active caspase-9 (~35 kDa) or active caspases-3, -6, and -7 (~21, 19, and 17 kDa). Affinity enrichment of biotinylated proteins followed by anticaspase blotting also suggested our probe did not label cellular caspases (Figure S2). To ensure that the apoptotic program had in fact

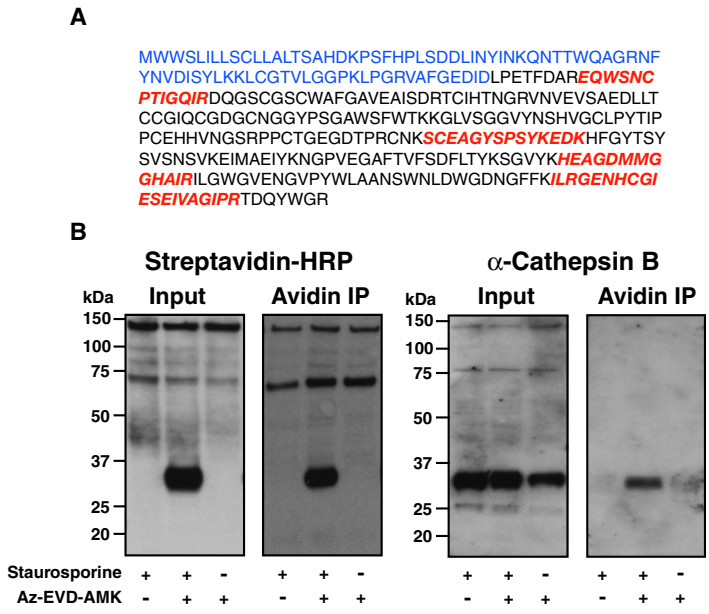

Figure 3. Identification of the Target of Probe 1 by Streptavidin Affinity Purification

NIH 3T3 cells were treated with staurosporine (1 μM) followed by probe **1** (300 nM). The Staudinger ligation was performed and labeled proteins were enriched by incubation with streptavidin-agarose beads.

(A) CatB amino acid sequence with the propeptide highlighted in blue and peptides identified by mass spectrometry in red.

(B) Streptavidin and CatB western blot analysis of enriched proteomes.

been activated, the same precipitated lysates were examined using antibodies against caspase-3, -7, -8, and -9 (Figure 2A). Consistent with activation of the intrinsic pathway, caspases-3, -7, and -9, but not caspase-8, all showed proteolytic processing to their active forms.

We were concerned that the apparent lack of caspase labeling may stem from a low efficiency of the Staudinger ligation step. To explore this, we took advantage of an alternative bioorthogonal coupling reaction, the Huisgen 1,3-dipolar cycloaddition between an organic azide and an alkyne, which has been reported to be quantitative when compared to direct labeling methods (Speers et al., 2003). This reaction can be catalyzed by Cu(I) salts (Wang et al., 2003) and has seen great utility for the secondary labeling of several ABPs (Sieber et al., 2006; Speers et al., 2003; Speers and Cravatt, 2004). Probe **3** (Ak-EVD-AMK; Figure 2B) was synthesized in a similar fashion as **1**, bearing an alkyne reactive handle in place of the azide. The alkyne of **3** presents an alternative reactivity profile, when compared to the azide, and will for example be resistant to conditions that may reduce the azide of **1** (Agard et al., 2006). NIH 3T3 cells were treated with staurosporine (1 μM) followed by probe **3** (300 nM) for 30 min. Following cell lysis, alkyne-bearing proteins were reacted with azido-biotin **4** under copper catalyzed cycloaddition conditions. Western blot analysis again showed biotin labeling of only one band at ~30 kDa in apoptotic cells, despite that fact that caspases had been activated by the staurosporine treatment (Figure 2B). We also performed a similar labeling experiment with probe **3** in which an azido-rhodamine derivative was used in the secondary labeling step (Charron et al., 2009). In this case the labeled proteins can be visualized by direct fluorescence imaging as opposed to western blotting. This allows us to explore if the problem stems from an inability of streptavidin-HRP to recognize the biotin moiety in the context of the labeled caspases. Once again, however, we observed labeling of a single ~30 kDa protein band in apoptotic cells but not in healthy cells (Figure S3).

Conceivably, steric hindrance within the enzyme active site could impede the secondary labeling reaction. To examine this possibility, NIH 3T3 cells were treated with staurosporine (1 μM) and **3** (300 nM) as above. The cells were collected, washed, lysed, and precipitated to denature the proteome. The precipitated proteins were then resuspended in a 4% SDS buffer and subjected to the cycloaddition conditions with azido biotin **4**. Under these labeling conditions we observed two bands at ~17 kDa (in addition to the 30 kDa band) corresponding to the expected molecular weight of the effector caspases-3 and -7 (Figure 2B and Figure S3). To further confirm the identity of these bands, we devised a competition experiment involving **1** and the commercially available biotin-VAD-fluoromethyl ketone, which can be used to label effector caspases following cell lysis. Pretreatment of apoptotic cells with increasing concentrations of **3** led to a dose-dependent block of effector caspase labeling by biotin-VAD-fluoromethyl ketone added after lysis (Figure S1B).

Identification of Probe-Labeled Protein

To determine the identity of the protein labeled by our probes under nondenaturing conditions, lysates from apoptotic NIH 3T3 cells prior treated with or without **1** were reacted with biotin probe **2** and incubated with streptavidin beads. Proteins captured on the beads were denatured and subjected to on-bead digestion by trypsin. Tryptic peptides eluted from streptavidin beads were collected and identified by tandem mass spectrometry (LC-MSMS). Assessment of eluted peptides revealed the cysteine protease CatB as the only protein present in probe-treated cells when compared to the control sample (Figure 3A). To confirm this result, streptavidin affinity enrichment was performed and analyzed by western blotting with a CatB-specific antibody (Figure 3B). Consistent with the mass spectrometric analysis, CatB was greatly enriched from apoptotic cells treated with probe **1** compared to healthy cells. As further validation, we found that probe **1** could label recombinant CatB in the presence of cell lysates and that no labeling was observed when CatB null (*catB*−/−) cells (from the corresponding knockout mouse) were treated with our probes (Figure S4).

Labeling of CatB was observed only in staurosporine-treated cells even though total levels of CatB in apoptotic and nonapoptotic cells remain constant (Figure 4A). This suggests that there is an alteration in the enzymatic activity following activation of the intrinsic apoptotic pathway. To see whether a similar phenomenon occurs upon activation of the extrinsic apoptotic cascade, we treated NIH 3T3 cells with cycloheximide (10 μg/mL) and

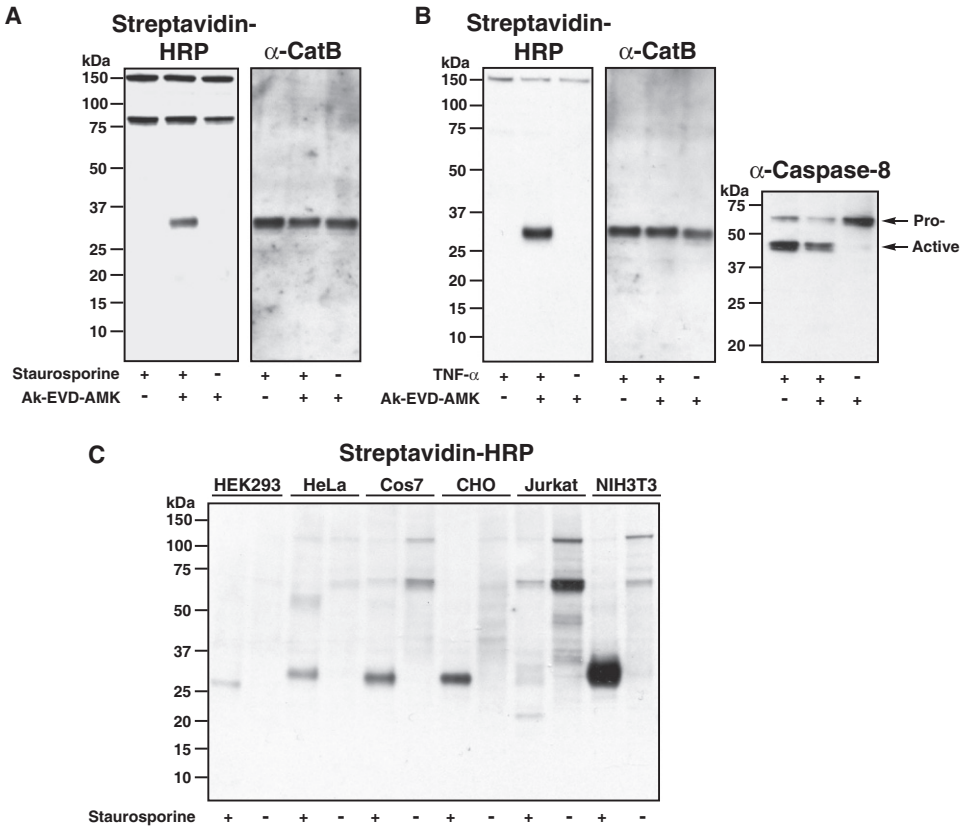

Figure 4. Streptavidin and CatB Western Blot Analysis of Probe 3 Labeling

(A) NIH 3T3 cells were treated with staurosporine (1 μM) followed by **3** (300 nM).

(B) NIH 3T3 cells were treated with TNF-α (10 ng/mL) and cycloheximide (10 μg/mL) followed by **3** (300 nM).

(C) A variety of cell lines were treated with staurosporine (1 μM) followed by **3**. In all cases cycloaddition reactions were performed with **4**, followed by streptavidin and western blotting.

tumor necrosis factor-α (TNF-α; 10 ng/mL) for 5 hr before addition of **3** to the media for 30 min. The cells were collected, subjected to cycloaddition conditions, and analyzed by western blotting (Figure 4B). We observed labeling of a single band consistent with CatB only in cells treated with TNF-α. Western blotting against caspase-8 indicated that the extrinsic pathway had indeed been initiated under these conditions (Figure 4B).

Although CatB has previously been implicated in TNF-α-induced apoptosis (Foghsgaard et al., 2001; Guicciardi et al., 2000, 2001), our data are the first evidence for a change in cellular CatB activity following initiation of the intrinsic pathway in intact cells. To ascertain whether this is a general phenomenon or one specific to NIH 3T3 cells, a panel of cell lines were treated with staurosporine (1 μM) followed by ABP **3** (300 nM) and biotin labeling with **4**. All cell types tested, with the exception of Jurkat cells, showed robust labeling of a protein, consistent with CatB upon treatment with staurosporine (Figure 4C). Thus, an alteration in cellular CatB activity, as reported by our APBs, appears to be a common feature of staurosporine-induced apoptosis. Next we asked whether other activators of the intrinsic pathway would also lead to an alteration in CatB activity. Accordingly, we treated NIH 3T3 cells with the topoisomerase II inhibitor, etoposide, followed by ABP **3** (300 nM) and biotin labeling with **4**. Consistent with the staurosporine studies, we observed labeling of a single ~30 kDa protein band in apoptotic cells and no labeling in healthy cells (Figure S5). Thus, we have identified conditions (i.e., treatment with low concentration of probe and secondary labeling under native folding conditions) in which probes **1** or **3** allow selective labeling of CatB upon activation of either the intrinsic or extrinsic apoptotic pathways.

Labeling of CatB Is Dependent on the Apoptotic Cascade

To determine if our activity-based probe is labeling CatB in an apoptosis-dependent manner and not as an indirect result of staurosporine treatment, we took advantage of immortalized mouse embryonic fibroblast (MEF) cells derived from caspase-9 null mice (Masud et al., 2007). Caspase-9 null MEF cells and wild-type MEF cells as a positive control (from knockout mice and wild-type littermates, respectively) were treated with staurosporine (1 μM) for 3 hr followed by treatment with probe **3** (300 nM) for 30 min. The cells were harvested, washed thoroughly, lysed, and labeled with azido-biotin **4** as above. As expected, western blot analysis showed labeling of a band of ~30 kDa in wild-type MEF cells corresponding to CatB (Figure 5). In contrast, little or no labeling of CatB was observed in the caspase-9 null MEF cells, despite equal amounts of protein as determined by anti-CatB blotting.

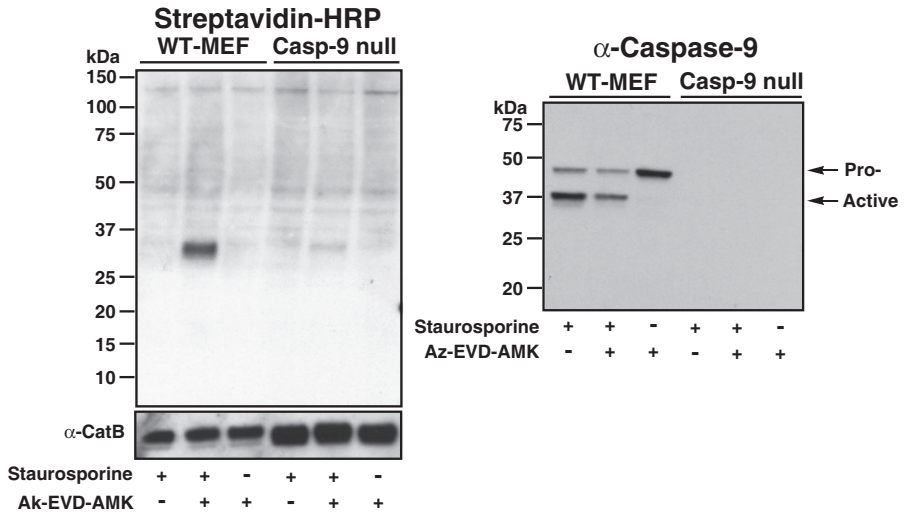

Figure 5. Probe Labeling of CatB in Caspase-9 Null Cells

Wild-type or caspase-9 null cells were treated with staurosporine (1 μM) to activate caspases. The cells were then treated with **3** (300 nM), followed by lysis, cycloaddition, and analysis by streptavidin and western blotting.

CatB Is Active at Cytosolic pH and Can Cleave Caspase Substrates

Several studies indicate that CatB, which normally resides in lysosomes, is released into the cytosol upon activation of the extrinsic apoptotic pathway (Foghsgaard et al., 2001; Guicciardi et al., 2000, 2001; Vancompernolle et al., 1998). We reasoned that our probe may be reporting on this relocalization of CatB and would therefore provide the first direct measurement of CatB activity in the cytosol during apoptosis. For this to be the case several criteria must be met: CatB must be active at cytosolic pH, our probes must be able to label CatB in the cytosol but not in the lysosome, and CatB must be released into the cytosol following activation of both the intrinsic and the extrinsic apoptotic pathways (since we see CatB labeling in both cases).

To address the first of these criteria, we measured the activity of purified CatB from human liver at pH 5 and 7 using both a cathepsin-directed peptide substrate (Z-Phe-Arg-AMC) as well as a panel of caspase substrates (Figure 6A). Although Z-Phe-Arg-AMC was the preferred substrate in this in vitro assay, CatB was found to cleave all of the caspase substrates tested. Moreover, this activity profile did not change appreciably between pH 4 and 7. These results are in good agreement with previous biochemical studies that indicate that CatB retains significant catalytic activity at pH 7 and can cleave, and be inhibited by, caspase-directed substrates and inhibitors, respectively (Foghsgaard et al., 2001; Khouri et al., 1991; Koga et al., 1991). Collectively, this data suggests that cytosolic CatB is able to cleave proteins with more prototypical cathepsin cleavage sites, as well as substrates containing caspase cleavage sites.

CatB Is Released into the Cytosol during Apoptosis where It Is Labeled by the Probe

Next we asked whether there is measurable CatB activity in the cytosol of apoptotic cells. NIH 3T3 cells were treated with staurosporine (1 μM) for 3 hr and a cytosolic fraction was then prepared using a digitonin extraction protocol (Foghsgaard et al., 2001). The remaining cell pellet was resuspended in NP-40 lysis buffer and centrifuged to provide a sample, termed NP40 soluble, enriched in organelles. These fractions were then assayed for cathepsin activity using the Z-Phe-Arg-AMC fluorescent substrate described above. An increase in cytosolic cathepsin activity was observed in staurosporine-treated cells compared to nonapoptotic cells (Figure 6B). Furthermore, this activity could be inhibited by the cathepsin inhibitor E64 (Barrett et al., 1982), ruling out caspase activity in our assay. Similar results were obtained using cytosolic fractions derived from NIH 3T3 cells treated with TNF-α (Figure S6).

With evidence of CatB release into the cytoplasm during apoptosis, we designed a competition assay to determine if our probe was indeed reporting on this relocalization. The cathepsin inhibitor E64 is not freely diffusible across cellular membranes and therefore unable to covalently modify cytosolically localized proteases in intact cells (Huang et al., 1992). However, it can access lysosomes through endocytosis and can therefore inhibit lysosomally localized cathepsins (Hang et al., 2006). This being the case, we reasoned that treatment of cells with E64 prior to addition of our probe should result in covalent inhibition of the entire lysosomal pool of CatB, resulting in a complete loss of labeling by **3**. Indeed, when NIH 3T3 cells were treated with E64 for 3 hr prior to either a selective concentration of **3** (300 nM) in apoptotic cells or a nonselective concentration of **3** (5 μM) in healthy cells, all CatB labeling was lost (Figure 6C). We interpret this result to mean that prior to the induction of apoptosis, CatB is localized to the lysosomes and covalently inhibited by E64.

This allowed us to perform a similar experiment by co-treating cells with E64 and probe **3**. We presumed that treatment of healthy cells with a high concentration of probe **3** (5 μM) leads to labeling of lysosomal CatB. Therefore co-treatment with an excess E64 (50 μM) should result in loss of probe **3** labeling, which was indeed the case (Figure 6C). In contrast, we

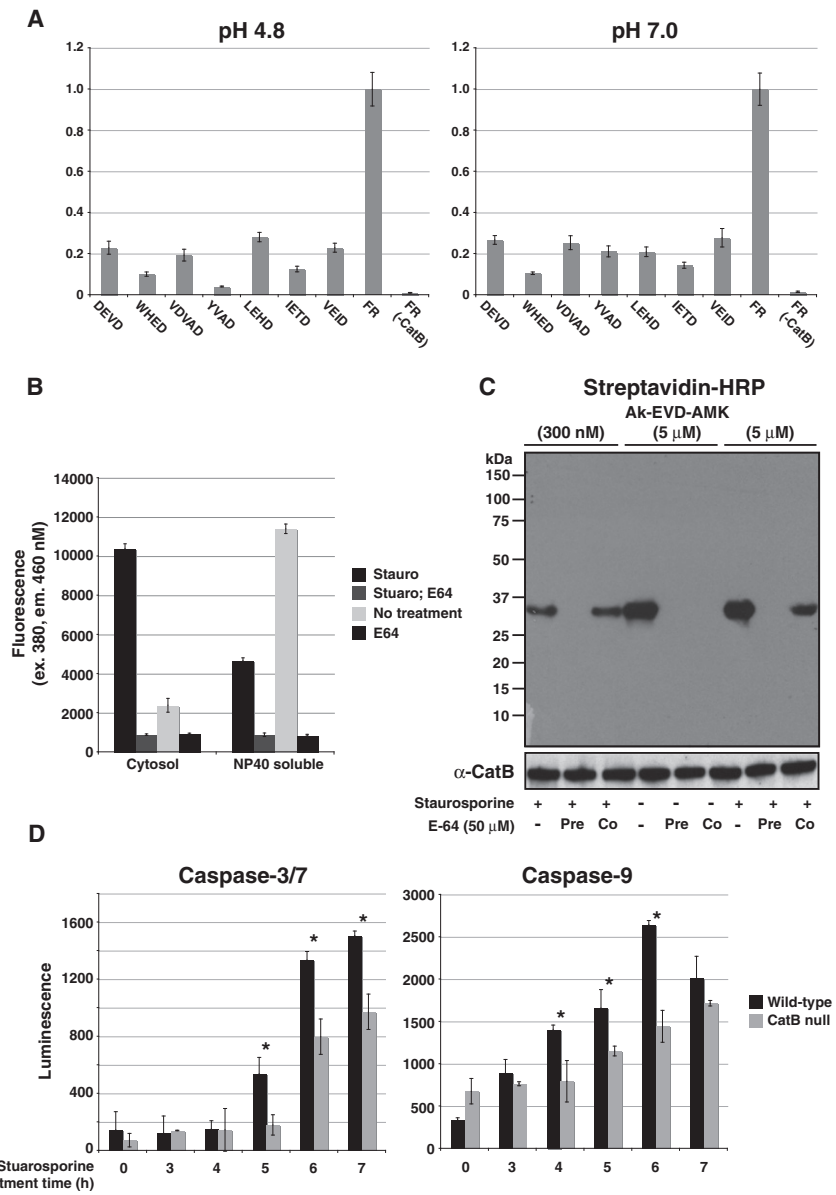

Figure 6. Probes 1 and 3 Read Out the Release of CatB into the Cytosol during Apoptosis

(A) CatB cleavage of caspase-like substrates at lysosomal and cytosolic pH. Purified CatB was incubated with several fluorogenic caspase peptide substrates for 30 min at 37°C and fluorescence of released amino-methylcoumarin (AMC; excitation at 380 nM; emission at 460 nM) was measured. Fluorescence was normalized to a canonical CatB substrate, Z-FR-AMC.

(B) Measurement of CatB activity in the cytosol during the intrinsic pathway of apoptosis. NIH 3T3 cells were treated with staurosporine (1 μM) or DMSO vehicle for 3 hr. The cytosol was then extracted with digitonin (labeled cytosol) and the remaining pellet was resuspended in NP-40 lysis buffer (labeled NP40 soluble). The fluorescent substrate Z-FR-AMC was then added and fluorescence was measured. The cathepsin inhibitor E64 inhibited the fluorescence signals.

(C) Competition of probe **3** labeling by the CatB inhibitor E64. NIH 3T3 cells were either pretreated with E64 (50 μM) for 1 hr prior to activation with staurosporine (1 μM) or DMSO vehicle for 3 hr. Staurosporine-treated cells were then treated with **3** alone (300 nM or 5 μM) or cotreated with **3** (300 nM or 5 μM) and E64 (50 μM) for 30 min prior to lysis and cycloaddition. Nonapoptotic cells were treated with **3** alone (5 μM) or cotreated with **3** (5 μM) and E64 (50 μM) for 30 min prior to lysis and cycloaddition. All samples were then analyzed by streptavidin blotting.

(D) Comparison of staurosporine-induced caspase activity in CatB null and wild-type fibroblasts. CatB null or wild-type fibroblasts were treated with staurosporine (1 μM) and caspase activity was measured at different treatment times using a caspase-dependent luminescence kit. Experiments in (A), (B), and (D) were performed in triplicate and errors are standard deviation (*$p < 0.05$, students t test).

presumed that treatment of apoptotic cells with a low concentration of probe **3** (300 nM) leads to labeling of mostly cytosolic CatB. This being the case, co-treatment with excess E64 should have little or no effect, which was our observation.

To ensure that E64 uptake is not simply impaired in apoptotic cells, we performed one additional experiment. We supposed that in apoptotic cells CatB resides in both the lysosome and cytosol and treatment with probe **3** at a high concentration (5 μM) will label both of these pools. If apoptotic cells can take up E64, co-treatment with excess E64 (50 μM) should result in loss of lysosomal labeling by probe **3**. The end result of this co-treatment would be labeling of solely the cytosolically localized CatB at a level similar to probe **3** at 300 nM, which is again what we observe (Figure 6C). Thus, the labeled CatB observed in apoptotic cells co-treated with probe **3** and E64 represents the cytosolic population of the protein.

CatB Is a Positive Regulator of the Intrinsic Apoptotic Cascade

CatB has been previously shown to be involved in crosstalk between the extrinsic and intrinsic apoptotic pathways (Guicciardi et al., 2000), where activation of caspase-8 by treatment with TNF-α resulted in the release of CatB from lysosomes. Furthermore, use of a cell-free system indicated that active caspase-8 could release CatB from purified lysosomes and that CatB, in turn, resulted in the activation of the intrinsic pathway through the release of cytochrome *c* from the mitochondria (Guicciardi et al., 2000). Consistent with this model, cells isolated from CatB null mice also showed diminished cytochrome *c* release, caspase activation, and apoptosis when treated with TNF-α (Guicciardi et al., 2000, 2001).

Because the intrinsic cell death pathway is typically initiated by the release of cytochrome *c*, we rationalized that CatB may be

acting in a positive feedback loop in staurosporine-induced apoptosis and set out to test that hypothesis. CatB null (*catB*−/−) and wild-type fibroblasts (from knockout mice and wild-type littermates, respectively) were treated with staurosporine (1 μM) and caspase-3 and -9 activities were measured at different times using an ex vivo caspase-dependent luminescence assay (Figure 6D). Both caspase-3 and -9 activities were diminished and delayed in CatB null cells when compared to wild-type controls. This suggests that CatB plays a role as a positive regulator not only in caspase-8-initiated cell death but also in the timely and efficient activation of the intrinsic apoptotic pathway.

DISCUSSION

We have described the serendipitous discovery of cell permeable activity-based probes that allow labeling of the lysosomal protease CatB in apoptotic cells. These probes were originally designed to visualize activated caspases via a two-step labeling scheme employing a bioorthogonal coupling reaction, either the Staudinger ligation or copper-catalyzed Huisgen cycloaddition. However, several lines of evidence including mass spectrometry and coimmunoprecipitation analyses (Figure 3) indicate that this labeling strategy instead results in the selective visualization of cytosolic CatB activity. Indeed, selective CatB labeling was observed in several different cell lines, regardless of the stimulus used to induce apoptosis (Figure 4). Activity probes that allow labeling of cathepsins (including CatB) in intact cells are known (Blum et al., 2005, 2007); however, selective visualization of CatB in apoptotic cells has not been reported previously.

That our probes should label CatB in cells is not entirely unexpected considering that previous studies have shown that caspase-targeted substrates and inhibitors can cross-react with CatB in vitro (Foghsgaard et al., 2001; Gray et al., 2001; Guicciardi et al., 2000, 2001; Rozman-Pungercar et al., 2003; Vancompernolle et al., 1998). More surprising was the lack of detectable caspase labeling in our initial cell-based experiments, particularly since probe **1** does label recombinant caspases added to cell lysates (Figure 1B). A likely explanation for this comes from our finding that endogenous effector caspases can be visualized when the secondary labeling reaction is performed under conditions expected to denature the cellular proteome (Figure 2B). This suggests that steric hindrance of the secondary labeling reaction in the caspase active site may be partly responsible for the lack of observable caspase labeling in the absence of denaturants. We propose that this steric problem, perhaps in combination with low levels of the activated caspases to begin with, places caspases below the detection threshold using our standard two-step labeling conditions. Presumably, CatB is above this threshold because it is more abundant and/or because the secondary labeling reaction is more efficient in this context. The net result of this is a labeling protocol for selectively visualizing CatB activity in apoptotic cells.

An ever-growing body of evidence has identified the CatB protease as an important participant in TNF-α-induced apoptosis (Foghsgaard et al., 2001; Guicciardi et al., 2000, 2001), and increase in CatB expression and activity initiates apoptosis in cells treated with an attenuated strain of *Mycobacterium bovis*, bacillus Calmette-Guérin (Sandes et al., 2007). Some small molecules and UVA/B light have also been shown to cause lysosomal permeabilization resulting in cathepsin-dependent cell death (Bivik et al., 2006; Droga-Mazovec et al., 2008; Yeung et al., 2006; Zhang et al., 2009). Additionally, staurosporine-induced apoptosis has been shown to be diminished in inclusion-cell disease fibroblasts, which have lowered levels of cathepsins B, D, and L (Terman et al., 2002). We have bolstered those results by providing the first direct measurement of CatB activity in the cytosol of intact apoptotic cells. We also provide direct evidence that CatB is released from lysosomes during the cell death pathway initiated by the intrinsic pathway in addition to the extrinsic apoptotic cascade (Figure 4). Interestingly, we did not observe CatB labeling in a MEF cell line lacking caspase-9, suggesting that release of CatB from lysosomes is downstream of the initiator caspase in the intrinsic pathway. Previous studies have indicated that caspase-8 is required for lysosomal release of CatB upon stimulation of the extrinsic pathway (Foghsgaard et al., 2001; Guicciardi et al., 2001). Indeed, it has been shown that recombinant caspase-8 can induce CatB release from purified lysosomes in a cell-free system (Guicciardi et al., 2000). Thus, it is possible that caspase-9 plays a similar role to caspase-8 in this lysosomal release phenomenon. Additional studies will be needed to further test this idea.

Upon induction of the intrinsic apoptotic pathway, we reasoned that CatB could be taking a role as a positive regulator of cell death by participating in a feed-forward activation loop, in addition to findings in previous reports that it can induce apoptosis. Feed-forward and -back loops are a hallmark of many biological signaling cascades whereby cells can tune their sensitivity to intra- and extracellular stimuli. The proteolytic cascade of caspase activation is a well-studied example of this. Caspase-9 is both an upstream activator and substrate of caspase-3, and the presence of caspase-3 has been shown to be essential for efficient activation of caspase-9 (Slee et al., 1999; Zou et al., 2003). We propose that CatB is a previously unidentified positive regulator of this important feedback machinery (Figure 7). One possible mechanism is CatB acting to reinforce the release of additional cytochrome *c*, thereby activating additional caspase-9. We have also showed that CatB is able to cleave peptides containing canonical caspase recognition sites (Figure 6A). Therefore, cytosolic CatB could also be directly activating caspases through proteolytic cleavage. Consistent with both hypotheses, CatB null cells treated with staurosporine show delayed and reduced activation of both caspase-9 and caspase-3 when compared to wild-type controls (Figure 6D). Further studies will be needed to test these ideas and to better understand the mechanism of the lysosomal release process generally. The ability to detect cytosolic CatB in intact cells using our probes should be helpful in this regard.

SIGNIFICANCE

The development of a cell-permeable cathepsin B (CatB) probe facilitated the further investigation into the role this important protease plays in cell death. Previous studies have relied upon indirect measurements and in vitro experimentation to visualize the release of CatB from lysosomes. The data presented here are the first direct visualization of

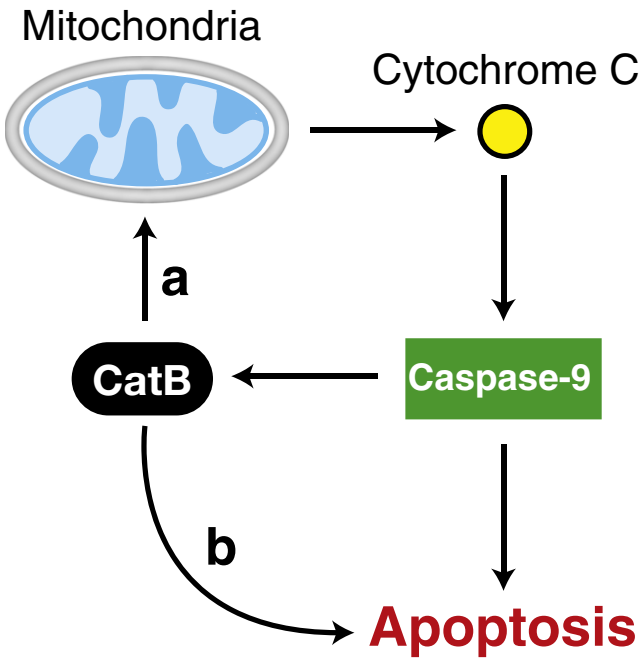

Figure 7. CatB as a Positive Regulator of the Intrinsic Apoptotic Cascade

Two nonmutually exclusive mechanisms are proposed. Active caspase-9 first results in release of CatB from the lysosome. In pathway a, cytosolic CatB results in the release of more cytochrome *c* from the mitochondria, reinforcing the activation of additional caspase-9. In addition, CatB can participate directly in apoptosis (pathway b) by proteolyzing proteins at canonical caspase cleavage sites.

this release into the cytosol in intact cells during apoptosis. We have used this chemical advance to explore a role for CatB in the intrinsic apoptotic pathway. Biochemical characterization of caspase-9 and CatB null cell lines places the release of CatB into the cytosol downstream of caspase-9, where it plays a role in the timely activation of the caspase proteolytic cascade. We hypothesize that CatB is acting through two nonmutually exclusive pathways. Mirroring its role in the crosstalk between the extrinsic and intrinsic apoptotic programs, CatB could release cytochrome *c* from the mitochondria resulting in further activation of caspase-9. Furthermore we have shown that CatB can cleave peptide substrates bearing canonical caspase recognition sequences, implicating CatB in the direct cleavage of caspase substrates. In summary, we propose that in addition to its previously understood role in apoptotic pathway crosstalk, CatB is an important member of the highly controlled feed-forward loop that ensures full caspase activation during intrinsically stimulated cell death.

EXPERIMENTAL PROCEDURES

All chemicals were obtained from commercial suppliers and were used as received unless otherwise noted. Staurosporine, E64, and Z-VAD-FMK were obtained from EMD Biosciences. Recombinant caspases and CatB purified from human liver were obtained from Biomol. Phosphine-biotin (**2**) was synthesized as previously described (Saxon and Bertozzi, 2000). PEO3-biotin was purchased from Pierce. Streptavidin-agarose and Softlink soft release avidin resin were purchased from Sigma and Promega, respectively. Caspase substrates were purchased from EMD Biosciences.

Probe Synthesis

Probes **1** and **3** were synthesized using commercially available amino acids and standard Fmoc solid phase peptide synthesis using DIC/HOBt coupling chemistry and modifications outlined in Kato et al. (2005a) Probes were then purified by RP-HPLC and identities were confirmed by ESI-MS; calculated for **1** $C_{50}H_{71}N_9O_{14}$ (M+H) 1022.51, found 1022.99; calculated for **3** $C_{51}H_{70}N_6O_{14}$ (M+H) 992.50, found 992.46.

Synthesis of Azido-biotin 4

Known azidovaleric acid (Seo et al., 2003) was activated to the corresponding pentafluorophenyl ester as follows. Azidovaleric acid (500 mg, 3.50 mmol) was dissolved in CH_2Cl_2 (5 mL) and pyridine (310 μL, 3.84 mmol) followed by pentafluorophenyl trifluoroacetate (690 μL, 4.00 mmol). The reaction was stirred for 45 min, washed with 1 N HCl, 10% $NaHCO_3$, and H_2O. The organic layer was dried over Na_2SO_4, filtered, and concentrated. This solid pink material (43 mg, 0.14 mmol) was added to a solution of PEO3-biotin (50 mg, 0.12 mmol) in DMF (2 mL) and the reaction was stirred for 16 hr. At this time the mixture was concentrated and the product purified by silica gel chromatography (7:2:1 ethyl acetate:MeOH:H_2O) to yield 53 mg (81%) as an off white powder. ^{1}H NMR (400 MHz, D_2O) δ 4.57 (dd, 1 H, J = 5.0, 7.8 Hz), 4.38 (dd, 1 H, J = 4.5, 7.8 Hz), 3.59 (app t, 6 H, J = 5.3 Hz), 3.35 (app t, 6 H, J = 5.2), 3.32–3.27 (m, 4 H), 2.95 (dd, 1 H, J = 5.0, 13.3 Hz), 2.74 (app d, 1 H, J = 13.0 Hz), 2.27–2.22 (m, 4 H), 1.74–1.52 (m, 8 H), 1.41–1.34 (m, 4 H); ^{13}C NMR (125 MHz, D_2O) δ 177.28, 176.98, 165.75, 70.11, 69.87, 69.32, 62.52, 60.69, 55.80, 51.81, 40.14, 39.35, 35.91, 35.63, 28.35, 28.15, 27.89, 25.58, 23.07; ESI-MS calculated for $C_{23}H_{41}N_7O_6S$ (M+H) 544.28, found 544.99.

Labeling of Recombinant Caspases

MCF7 cells, grown to confluency, were collected from a 10 cm dish by gentle scraping and pelleted by centrifugation at 2000 × g. After the cell pellet was washed with PBS (1 mL) two times, the cells were lysed in 200 μl of ice-cold NP lysis buffer (0.5% NP-40, 50 mM Tris, and 5 mM $MgCl_2$ [pH 7.4]) for 20 min and centrifuged at 4°C for 10 min at 10,000 × g. The supernatant (post-nuclear lysate) was collected and the protein concentration was determined by Bradford assay (Bio-Rad). Probe labeling of recombinant caspases was accomplished by incubation of MCF7 cell lysate (50 μg) with recombinant caspase (10 μL, 1000 U) and 1 μM probe **1** (1 mM in DMSO stock) in a total volume of 100 μl for 90 min at room temperature. The lysates were then concentrated using Vivaspin (Sartorius) 500 columns (10,000 MWCO PES) and washed with lysis buffer (500 μL). The resulting protein solutions were diluted with NP lysis buffer to a volume of 100 μl and subjected to the Staudinger ligation.

Live Cell Probe Treatment with Intrinsic Pathway Activation

NIH 3T3, wild-type MEFs, caspase-9 null MEFs, CatB null MEFs, CHO, Jurkat, HEK293, or HeLa cells at ~80%–90% confluency in a 10 cm dish were treated with serum-free media (10 mL) for 16 hr. At this time staurosporine (10 μL; 1 mM in DMSO) was added to give a final concentration of 1 μM (DMSO vehicle was added to all control plates). After 3 hr the cells were treated with probes **1** or **3** (0.1 to 50 μM; 1000× in DMSO stock) or DMSO for 30 min. Alternatively, cells were activated with etoposide (10 μM) and cycloheximide (10 μg/mL) for 12 hr. The cells were then collected by gentle scraping and pelleted by centrifugation at 2000 × g, followed by washing with PBS (1 mL) two times. Cell pellets from ~2.0×10^7 cells were resuspended in 100 μl of ice-cold NP lysis buffer (0.5% NP-40, 50 mM Tris, and 5 mM $MgCl_2$ [pH 7.4]) with Complete Mini protease inhibitor cocktail (Roche Biosciences) for 30 min and then centrifuged at 4°C for 10 min at 10,000 × g. The supernatant (total cell lysate) was collected and the protein concentration was determined by Bradford assay.

Extrinsic Pathway Activation

NIH 3T3 cells at ~80%–90% confluency in a 10 cm dish were treated with cycloheximide (10 μg/mL; 10 mg/mL stock in H_2O) and TNF-α (10 ng/mL) for 5 hr. At this time, probe **1** (300 nM) was added for 30 min and the cells were processed as above.

Labeling of Cell Lysates by Staudinger Ligation

Staudinger ligation labeling of azide-modified proteins was performed by incubation of post-nuclear lysates (100 μg) with 250 μM of phosphine-biotin (**2**; 5 mM in DMSO stock) and 5 mM dithiothreitol (50 mM in H_2O stock) in a total reaction volume of 100 μl for 2 hr at 37°C. The reactions were terminated by addition of ice-cold acetone (1 mL), incubated at −20°C for 20 min, and centrifuged at 4°C for 10 min at 18,000 × g to precipitate proteins. The supernatant was careful decanted and the resulting pellet dried at room temperature for 5 min to remove any excess acetone. The protein pellet was subsequently resuspended in SDS-protein loading buffer with 2-mercaptoethanol and boiled for 10 min.

Labeling of Cell Lysates by Cycloaddition

Cells lysates (100 μg) were prepared with modified NP-40 lysis buffer (1% NP-40, 50 mM triethanolamine, and 150 mM NaCl [pH 7.4]) with Complete Mini protease inhibitor cocktail (Roche Biosciences) and cycloaddition reactions were performed as follows. Azido-biotin tag (**4**; 100 μM; 5 mM stock in DMSO) or azido-rhodamine (100 μM; 5 mM stock in DMSO) was added, followed by 1 mM TCEP (50 mM stock in H_2O) and 100 μM triazole ligand (Speers and Cravatt, 2004) (1.7 mM stock in DMSO/t-butanol 1:4). The samples were gently vortexed and 1 mM $CuSO_4$ (50 mM stock in H_2O) was added. Samples were vortexed again and allowed to reaction at room temperature for 1 hr. At this time, the reactions were terminated by addition of ice-cold acetone (1 mL), incubated at −20°C for 20 min, and centrifuged at 4°C for 10 min at 18,000 × g to precipitate proteins. The supernatant was careful decanted and the resulting pellet dried at room temperature for 5 min to remove any excess acetone. The protein pellet was subsequently resuspended in SDS-protein loading buffer with 2-mercaptoethanol and boiled for 10 min.

Denaturation of Cellular Proteome

NIH cells, grown to confluency and treated with staurosporine and **3** as above, were collected from a 10 cm dish by gentle scraping and pelleted by centrifugation at 2000 × g. After the cell pellet was washed with PBS (1 mL) two times, the cells were lysed in 200 μl of ice-cold modified NP lysis buffer (1% NP-40, 50 mM triethanolamine, and 150 mM NaCl [pH 7.4]) for 20 min and centrifuged at 4°C for 10 min at 10,000 × g. The supernatant (post-nuclear lysate) was collected and the protein concentration was determined by Bradford assay (Bio-Rad). The 200 μg of total protein were then precipitated by addition of ice-cold acetone (1 mL) and incubation at −20°C for 30 min. After centrifugation at 10,000 × g for 10 min and careful decanting, the precipitated proteins were resuspended in SDS buffer (100 μl; 4% SDS, 50 mM triethanolamine, and 150 mM NaCl [pH 7.4]) and subjected to the cycloaddition conditions.

Streptavidin Affinity Enrichment of Biotinylated Proteins

Cell lysates (10 mg for mass spectroscopic analysis or 1/10 scale for western blot analysis) from NIH 3T3 cells treated with **1** as above were reacted with 25 μM of **2** (5 mM in DMSO stock) and 5 mM dithiothreitol (50 mM in H_2O stock) in a total reaction volume of 10 ml at 37°C with rocking. The reactions were terminated by the addition of ice-cold acetone (40 mL), incubated at −20°C for 20 min, and centrifuged at 4°C for 10 min at 10,000 × g to precipitate proteins. The supernatant was decanted and the protein pellet was resuspended in 10 ml of 0.2% SDS and 50 mM Tris (pH 7.4) with sonication. Proteins were precipitated again with ice-cold acetone (40 mL) and resuspended in 0.2% SDS and 50 mM Tris (pH 7.4) with sonication to remove any residual **2**. Prewashed streptavidin-agarose beads (250 μL; for mass spectroscopic analysis) or Softlink soft release avidin resin (25 μL; for western blot analysis) were then added to resuspended protein lysates (1 mg/mL) and allowed to incubate at 4°C for 1 hr with rocking. The beads were centrifuged for 5 min at 4000 × g at 4°C and washed with 10 ml of 0.2% SDS and 50 mM Tris (pH 7.4) four times.

Proteomic Analysis of Biotinylated Proteins

Washed streptavidin-agarose beads (~250 μL) were washed twice with 1 ml of 50 mM triethylammonium bicarbonate (pH 7.4). Attached proteins were then denatured and reduced with 500 μl of 6 M urea, 10 mM TCEP, and 50 mM triethylammonium bicarbonate (pH 7.4) for 30 min at room temperature with rocking. Iodoacetamide from a stock solution of 1 M was added to this slurry to give a final concentration of 20 mM iodoacetamide and was allowed to react for 30 min at room temperature with rocking in the dark. The beads were then washed with 1 ml of 50 mM triethylammonium bicarbonate (pH 7.4) three times, resuspended in 500 μl of 50 mM triethylammonium bicarbonate (pH 7.4) with 2 μg of porcine trypsin, and allowed to digest overnight at 37°C with rocking. The beads were centrifuged for 1 min at 4000 × g, and the supernatants were collected and concentrated to a volume of ~15 μl by speedvac. Glacial acetic acid was added to stop digestion and adjust the pH of the solution to 3.5. The sample was pressure loaded directly onto a 360 × 75 μm PicoFrit column equipped with a 15 μm tip and a 5 cm bed of BioBasic C18 material (New Objective, Inc.). Subsequently the sample was analyzed on a Finnigan LTQ (Thermo Fisher Scientific) in positive electrospray mode using a linear gradient of 0%–100% B over 90 min (A = 0.1 M acetic acid in nanopure water, B = 70% acetonitrile in 0.1 M acetic acid) and a flow rate of 150 nL/min on a Smart System HPLC (Pharmacia). The spectra were acquired with the instrument operating in data-dependent mode. A full scan mass spectrum was followed by 10 MS/MS spectra on the ten most abundant ions. The isolation window for precursor selection was set to ±1.5 Da, the collision energy to 35%, and the activation Q was set to 0.25. The target value for the full scan was set to 3e4 and for the MS/MS scan to 1e4. The selected ions were set on a dynamic exclusion list for 30 s, except predicted tryptic peptides of avidin were set on a static exclusion list. The MS/MS data was analyzed by using the open source search engine, X! Tandem (version 2007.01.01), to search the spectra against the NCBI database using the X! Hunter search algorithm. Searches were limited to the *Mus musculus* genome, and the parameters were set to a fragment mass error of ±0.4 Da. Four tryptic peptides covering ~25% of CatB were identified from the fragmentation data. The base-10 log of the expectation value was −97.4, signifying a high confidence that CatB was present in the sample. No CatB peptides were identified from a control sample of apoptotic NIH 3T3 cells that had not been treated with probe **1**.

Labeling of CatB In Vitro

Purified CatB (1.5 μg; Biomol) was added to BSA (100 μg) and Jurkat cell lysate (2 mg/mL; modified NP-40 lysis buffer), 100 μl total volume. DMSO vehicle or probe **3** (500 μM stock in DMSO; 1 μM final concentration) was then added. After 1 hr at room temperature, the reaction was terminated by addition of ice-cold acetone followed by incubation at −20°C for 20 min. The resulting precipitated proteins were centrifuged at 18,000 × g and the supernatant was carefully decanted. The protein pellet was washed with ice-cold acetone twice and then resolubilized in 100 μl of 4% SDS, 50 mM triethanolamine, and 150 mM NaCl (pH 7.4). Cycloadditions were then performed as above.

Western Blotting

Biotin (~25 μg) labeled proteins were separated by SDS-PAGE and transferred to a PVDF membrane and the membrane was blocked with 5% nonfat dried milk in TBST (50 mM Tris, 150 mM NaCl, and 0.5% Tween 20 [pH 7.6]) overnight at 4°C or 1 hr at room temperature. The membrane was washed with TBST for 10 min (3 × 20 mL) and incubated with streptavidin-HRP (GE Healthcare; 1:5000 in TBST) for 1 hr. The membrane was washed again with TBST for 10 min (3 × 20 mL) and developed using ECL reagents (PerkinElmer) and Kodak Biomax MR film. To ascertain levels of endogenous proteins in Figure 2, equal amounts of protein were run and probed with anti-caspase antibodies. In all other figures the above membranes were stripped and blocked as above, and then probed with anti-caspase antibodies (Cell Signaling Technologies; 1:1000), an anti-CatB antibody (Santa Cruz Biotechnology; 1:300), or an anti-PARP antibody (BD PharMingen; 1:1000). After washing three times with TBST, the blots were incubated with HRP-conjugated secondary antibodies (GE Healthcare) for 1 hr in blocking buffer, washed three more times with TBST, and developed using ECL reagents (PerkinElmer) and Kodak Biomax MR film.

In Vitro Activity Assay

AMC derivatized peptide substrates (DMSO stocks) were added to an imidazole-HCl buffer (pH 4.8 or 7.0) (100 μL) containing 8 mM dithiothreitol and 4 mM EDTA. A solution of CatB (200 ng/μL) in 0.1% Brij 35 solution (5 μL) was then added. After incubating for 30 min at 37°C, the reaction was terminated by addition of 100 mM sodium chloroacetate in 100 mM sodium acetate buffer (pH 4.3) (150 μL). Fluorescence (excitation at 380 nM; emission at 460 nM) was then measured.

Measurement of Cytosolic CatB Activity

NIH 3T3 cells were either activated for apoptosis with staurosporine or TNF-α as above or left untreated. The cells were then collected by gentle scraping and pelleted by centrifugation at 2000 × g, followed by washing with PBS (1 mL) two times. Cells were treated with 25 μg/mL digitonin, 20 mM triethanolamine, and 10 mM KCl_2 for 10 min. After centrifugation at 10,000 × g for 10 min the supernatant was collected, which contains the cytosolic fraction. The pellet was then suspended in modified NP lysis buffer followed by centrifugation at 10,000 × g for 10 min. The resulting supernatant contains the NP-40 soluble fraction. Total protein from each fraction (30 μg) was normalized and then added to an imidazole-HCl buffer (pH 4.8) (100 μL) containing 8 mM dithiothreitol and 4 mM EDTA and was either treated with the cathepsin inhibitor E64 (200 μM) or with DMSO vehicle for 30 min. At this time Z-Phe-Arg-AMC was added to give a final concentration of 200 μM and the reactions were incubated at 37°C for 30 min. Fluorescence (excitation at 380 nM; emission at 460 nM) was then measured. All experiments were performed in triplicate.

E64 Competition Experiment

NIH 3T3 cells were either pretreated with E64 (50 μM) for 1 hr prior to activation with staurosporine (1 μM) or DMSO vehicle for 3 hr. Staurosporine-treated cells were then treated with **3** alone (300 nM or 5 μM) or cotreated with **3** (300 nM or 5 μM) and E64 (50 μM) for 30 min prior to lysis and the cycloaddition conditions described above. Nonapoptotic cells were treated with **3** alone (5 μM) or cotreated with **3** (5 μM) and E64 (50 μM) for 30 min prior to lysis and the cycloaddition conditions.

Measurement of Caspase Activity in CatB Null Cells

CatB null or the corresponding wild-type MEFs (~25,000 per well) were plated in a white plate, clear bottom 96 well assay plate (Corning Incorporated). After 16 hr the cells were washed with PBS and 100 μl media containing staurosporine (1 μM) was added. At the indicated times, 100 μl of Caspase-Glo 3/7 or Caspase-Glo 9 assay (Promega) was added to the appropriate wells. The mixtures were incubated for 45 min and luminescence was measured according to the manufacturer's directions using a 96 well luminometer (Molecular Biosystems).

SUPPLEMENTAL DATA

Supplemental Data include Supplemental Experimental Procedures, one scheme, and six figures and can be found with this article online at http://www.cell.com/chemistry-biology/supplemental/S1074-5521(09)00243-9.

ACKNOWLEDGMENTS

We thank M. Bader and E.C. Schwartz for helpful discussions, Howard C. Hang (Rockefeller University) for azido-rhodamine, Bonnie F. Sloane (Wayne State University) for wild-type and CatB null MEFs from the corresponding knockout mice (C57BL/6J genetic background), and Richard Flavell (Yale Medical School) for wild-type and caspase-9 null MEFs from the corresponding knockout mice (C57BL/6J genetic background). We also thank Brian T. Chait (Rockefeller University) for access to mass spectrometers. We acknowledge National Institutes of Health (NIH) grants (EB001991 and GM072015) to T.W.M., NIH grant (RR00862) to B.T. Chait, and American Cancer Society postdoctoral fellowships to M.R.P. and K.P.C. for research support.

Received: April 30, 2009
Revised: June 26, 2009
Accepted: July 23, 2009
Published: September 24, 2009

REFERENCES

Agard, N.J., Baskin, J.M., Prescher, J.A., Lo, A., and Bertozzi, C.R. (2006). A comparative study of bioorthogonal reactions with azides. ACS Chem. Biol. *1*, 644–648.

Barrett, A.J., Kembhavi, A.A., Brown, M.A., Kirschke, H., Knight, C.G., Tamai, M., and Hanada, K. (1982). L-trans-Epoxysuccinyl-leucylamido(4-guanidino)-butane (E-64) and its analogues as inhibitors of cysteine proteinases including cathepsins B, H and L. Biochem. J. *201*, 189–198.

Berger, A.B., Witte, M.D., Denault, J.B., Sadaghiani, A.M., Sexton, K.M., Salvesen, G.S., and Bogyo, M. (2006). Identification of early intermediates of caspase activation using selective inhibitors and activity-based probes. Mol. Cell *23*, 509–521.

Bivik, C.A., Larsson, P., Kågedal, K., Rosdahl, I., and Öllinger, K. (2006). UVA/B-induced apoptosis in human melanocytes involves translocation of cathepsins and Bcl-2 family members. J. Invest. Dermatol. *126*, 1119–1127.

Blum, G., Mullins, S.R., Keren, K., Fonovic, M., Jedeszko, C., Rice, M.J., Sloane, B.F., and Bogyo, M. (2005). Dynamic imaging of protease activity with fluorescently quenched activity-based probes. Nat. Chem. Biol. *1*, 203–209.

Blum, G., von Degenfeld, G., Merchant, M.J., Blau, H.M., and Bogyo, M. (2007). Noninvasive optical imaging of cysteine protease activity using fluorescently quenched activity-based probes. Nat. Chem. Biol. *3*, 668–677.

Charron, G., Zhang, M.M., Yount, J.S., Wilson, J., Raghavan, A.S., Shamir, E., and Hang, H.C. (2009). Robust fluorescent detection of protein fatty-acylation with chemical reporters. J. Am. Chem. Soc. *131*, 4967–4975.

Danial, N.N., and Korsmeyer, S.J. (2004). Cell death: critical control points. Cell *116*, 205–219.

Denault, J.B., Bekes, M., Scott, F.L., Sexton, K.M., Bogyo, M., and Salvesen, G.S. (2006). Engineered hybrid dimers: tracking the activation pathway of caspase-7. Mol. Cell *23*, 523–533.

Deveraux, Q.L., Stennicke, H.R., Salvesen, G.S., and Reed, J.C. (1999). Endogenous inhibitors of caspases. J. Clin. Immunol. *19*, 388–398.

Dix, M.M., Simon, G.M., and Cravatt, B.F. (2008). Global mapping of the topography and magnitude of proteolytic events in apoptosis. Cell *134*, 679–691.

Droga-Mazovec, G., Bojic, L., Petelin, A., Ivanova, S., Romih, R., Repnik, U., Salvesen, G., Stoka, V., Turk, V., and Turk, B. (2008). Cysteine cathepsins trigger caspase-dependent cell death through cleavage of bid and antiapoptotic Bcl-2 homologues. J. Biol. Chem. *283*, 19140–19150.

Foghsgaard, L., Wissing, D., Mauch, D., Lademann, U., Bastholm, L., Boes, M., Elling, F., Leist, M., and Jaattela, M. (2001). Cathepsin B acts as a dominant execution protease in tumor cell apoptosis induced by tumor necrosis factor. J. Cell Biol. *153*, 999–1010.

Gocheva, V., Zeng, W., Ke, D., Klimstra, D., Reinheckel, T., Peters, C., Hanahan, D., and Joyce, J.A. (2006). Distinct roles for cysteine cathepsin genes in multistage tumorigenesis. Genes Dev. *20*, 543–556.

Gray, J., Haran, M.M., Schneider, K., Vesce, S., Ray, A.M., Owen, D., White, I.R., Cutler, P., and Davis, J.B. (2001). Evidence that inhibition of cathepsin-B contributes to the neuroprotective properties of caspase inhibitor Tyr-Val-Ala-Asp-chloromethyl ketone. J. Biol. Chem. *276*, 32750–32755.

Green, D.R., and Evan, G.I. (2002). A matter of life and death. Cancer Cell *1*, 19–30.

Guicciardi, M.E., Deussing, J., Miyoshi, H., Bronk, S.F., Svingen, P.A., Peters, C., Kaufmann, S.H., and Gores, G.J. (2000). Cathepsin B contributes to TNF-alpha-mediated hepatocyte apoptosis by promoting mitochondrial release of cytochrome c. J. Clin. Invest. *106*, 1127–1137.

Guicciardi, M.E., Miyoshi, H., Bronk, S.F., and Gores, G.J. (2001). Cathepsin B knockout mice are resistant to tumor necrosis factor-alpha-mediated hepatocyte apoptosis and liver injury: implications for therapeutic applications. Am. J. Pathol. *159*, 2045–2054.

Hanahan, D., and Weinberg, R.A. (2000). The hallmarks of cancer. Cell *100*, 57–70.

Hang, H.C., Loureiro, J., Spooner, E., van der Velden, A.W., Kim, Y.M., Pollington, A.M., Maehr, R., Starnbach, M.N., and Ploegh, H.L. (2006). Mechanism-based probe for the analysis of cathepsin cysteine proteases in living cells. ACS Chem. Biol. *1*, 713–723.

Huang, Z., McGowan, E.B., and Detwiler, T.C. (1992). Ester and amide derivatives of E64c as inhibitors of platelet calpains. J. Med. Chem. *35*, 2048–2054.

Jedeszko, C., and Sloane, B.F. (2004). Cysteine cathepsins in human cancer. Biol. Chem. *385*, 1017–1027.

Kato, D., Boatright, K.M., Berger, A.B., Nazif, T., Blum, G., Ryan, C., Chehade, K.A.H., Salvesen, G.S., and Bogyo, M. (2005a). Activity-based probes that target diverse cysteine protease families. Nat. Chem. Biol. *1*, 33–38.

Kato, D., Verhelst, S.H., Sexton, K.B., and Bogyo, M. (2005b). A general solid phase method for the preparation of diverse azapeptide probes directed against cysteine proteases. Org. Lett. *7*, 5649–5652.

Khouri, H.E., Plouffe, C., Hasnain, S., Hirama, T., Storer, A.C., and Menard, R. (1991). A model to explain the pH-dependent specificity of cathepsin B-catalysed hydrolyses. Biochem. J. *275*, 751–757.

Kirkegaard, T., and Jaattela, M. (2009). Lysosomal involvement in cell death and cancer. Biochim. Biophys. Acta *1793*, 746–754.

Koga, H., Yamada, H., Nishimura, Y., Kato, K., and Imoto, T. (1991). Multiple proteolytic action of rat liver cathepsin B: specificities and pH-dependences of the endo- and exopeptidase activities. J. Biochem. *110*, 179–188.

Lin, F.L., Hoyt, H.M., van Halbeek, H., Bergman, R.G., and Bertozzi, C.R. (2005). Mechanistic investigation of the staudinger ligation. J. Am. Chem. Soc. *127*, 2686–2695.

Mahrus, S., Trinidad, J.C., Barkan, D.T., Sali, A., Burlingame, A.L., and Wells, J.A. (2008). Global sequencing of proteolytic cleavage sites in apoptosis by specific labeling of protein N termini. Cell *134*, 866–876.

Masud, A., Mohapatra, A., Lakhani, S.A., Ferrandino, A., Hakem, R., and Flavell, R.A. (2007). Endoplasmic reticulum stress-induced death of mouse embryonic fibroblasts requires the intrinsic pathway of apoptosis. J. Biol. Chem. *282*, 14132–14139.

Mohamed, M.M., and Sloane, B.F. (2006). Cysteine cathepsins: multifunctional enzymes in cancer. Nat. Rev. Cancer *6*, 764–775.

Rathmell, J.C., and Thompson, C.B. (2002). Pathways of apoptosis in lymphocyte development, homeostasis, and disease. Cell *109* (*Suppl*), S97–S107.

Riedl, S.J., and Shi, Y. (2004). Molecular mechanisms of caspase regulation during apoptosis. Nat. Rev. Mol. Cell Biol. *5*, 897–907.

Roshy, S., Sloane, B.F., and Moin, K. (2003). Pericellular cathepsin B and malignant progression. Cancer Metastasis Rev. *22*, 271–286.

Rozman-Pungercar, J., Kopitar-Jerala, N., Bogyo, M., Turk, D., Vasiljeva, O., Stefe, I., Vandenabeele, P., Bromme, D., Puizdar, V., Fonovic, M., et al. (2003). Inhibition of papain-like cysteine proteases and legumain by caspase-specific inhibitors: when reaction mechanism is more important than specificity. Cell Death Differ. *10*, 881–888.

Saftig, P., Hunziker, E., Wehmeyer, O., Jones, S., Boyde, A., Rommerskirch, W., Moritz, J.D., Schu, P., and von Figura, K. (1998). Impaired osteoclastic bone resorption leads to osteopetrosis in cathepsin-K-deficient mice. Proc. Natl. Acad. Sci. USA *95*, 13453–13458.

Salvesen, G.S. (2001). A lysosomal protease enters the death scene. J. Clin. Invest. *107*, 21–22.

Sandes, E., Lodillinsky, C., Cwirenbaum, R., Arguelles, C., Casabe, A., and Eijan, A.M. (2007). Cathepsin B is involved in the apoptosis intrinsic pathway induced by Bacillus Calmette-Guérin in transitional cancer cell lines. Int. J. Mol. Med. *20*, 823–828.

Saxon, E., and Bertozzi, C.R. (2000). Cell surface engineering by a modified Staudinger reaction. Science *287*, 2007–2010.

Schraufstatter, I.U., Trieu, K., Zhao, M., Rose, D.M., Terkeltaub, R.A., and Burger, M. (2003). IL-8-mediated cell migration in endothelial cells depends on cathepsin B activity and transactivation of the epidermal growth factor receptor. J. Immunol. *171*, 6714–6722.

Seo, T.S., Li, Z., Ruparel, H., and Ju, J. (2003). Click chemistry to construct fluorescent oligonucleotides for DNA sequencing. J. Org. Chem. *68*, 609–612.

Shi, G.P., Villadangos, J.A., Dranoff, G., Small, C., Gu, L., Haley, K.J., Riese, R., Ploegh, H.L., and Chapman, H.A. (1999). Cathepsin S required for normal MHC class II peptide loading and germinal center development. Immunity *10*, 197–206.

Sieber, S.A., Niessen, S., Hoover, H.S., and Cravatt, B.F. (2006). Proteomic profiling of metalloprotease activities with cocktails of active-site probes. Nat. Chem. Biol. *2*, 274–281.

Slee, E.A., Harte, M.T., Kluck, R.M., Wolf, B.B., Casiano, C.A., Newmeyer, D.D., Wang, H.G., Reed, J.C., Nicholson, D.W., Alnemri, E.S., et al. (1999). Ordering the cytochrome c-initiated caspase cascade: hierarchical activation of caspases-2, -3, -6, -7, -8, and -10 in a caspase-9-dependent manner. J. Cell Biol. *144*, 281–292.

Speers, A.E., and Cravatt, B.F. (2004). Profiling enzyme activities in vivo using click chemistry methods. Chem. Biol. *11*, 535–546.

Speers, A.E., Adam, G.C., and Cravatt, B.F. (2003). Activity-based protein profiling in vivo using a copper(i)-catalyzed azide-alkyne [3 + 2] cycloaddition. J. Am. Chem. Soc. *125*, 4686–4687.

Stennicke, H.R., Deveraux, Q.L., Humke, E.W., Reed, J.C., Dixit, V.M., and Salvesen, G.S. (1999). Caspase-9 can be activated without proteolytic processing. J. Biol. Chem. *274*, 8359–8362.

Terman, A., Neuzil, J., Kagedal, K., Ollinger, K., and Brunk, U.T. (2002). Decreased apoptotic response of inclusion-cell disease fibroblasts: a consequence of lysosomal enzyme missorting? Exp. Cell Res. *274*, 9–15.

Turk, B., Stoka, V., Rozman-Pungercar, J., Cirman, T., Droga-Mazovec, G., Oresic, K., and Turk, V. (2002). Apoptotic pathways: involvement of lysosomal proteases. Biol. Chem. *383*, 1035–1044.

Vancompernolle, K., Van Herreweghe, F., Pynaert, G., Van de Craen, M., De Vos, K., Totty, N., Sterling, A., Fiers, W., Vandenabeele, P., and Grooten, J. (1998). Atractyloside-induced release of cathepsin B, a protease with caspase-processing activity. FEBS Lett. *438*, 150–158.

Vaux, D.L., and Flavell, R.A. (2000). Apoptosis genes and autoimmunity. Curr. Opin. Immunol. *12*, 719–724.

Wang, Q., Chan, T.R., Hilgraf, R., Fokin, V.V., Sharpless, K.B., and Finn, M.G. (2003). Bioconjugation by copper(I)-catalyzed azide-alkyne [3 + 2] cycloaddition. J. Am. Chem. Soc. *125*, 3192–3193.

Yang, X.H., Sladek, T.L., Liu, X., Butler, B.R., Froelich, C.J., and Thor, A.D. (2001). Reconstitution of caspase 3 sensitizes MCF-7 breast cancer cells to doxorubicin- and etoposide-induced apoptosis. Cancer Res. *61*, 348–354.

Yeung, B.H., Huang, D.C., and Sinicrope, F.A. (2006). PS-341 (bortezomib) induces lysosomal cathepsin B release and a caspase-2-dependent mitochondrial permeabilization and apoptosis in human pancreatic cancer cells. J. Biol. Chem. *281*, 11923–11932.

Yuan, J., and Yankner, B.A. (2000). Apoptosis in the nervous system. Nature *407*, 802–809.

Zhang, H., Zhong, C., Shi, L., Guo, Y., and Fan, Z. (2009). Granulysin induces cathepsin B release from lysosomes of target tumor cells to attack mitochondria through processing of bid leading to Necroptosis. J. Immunol. *182*, 6993–7000.

Zheng, T.S., Hunot, S., Kuida, K., and Flavell, R.A. (1999). Caspase knockouts: matters of life and death. Cell Death Differ. *6*, 1043–1053.

Zou, H., Yang, R., Hao, J., Wang, J., Sun, C., Fesik, S.W., Wu, J.C., Tomaselli, K.J., and Armstrong, R.C. (2003). Regulation of the Apaf-1/caspase-9 apoptosome by caspase-3 and XIAP. J. Biol. Chem. *278*, 8091–8098.

